Structure, Stability, and Reactivity of Cationic Hydrogen Trioxides and Thermochemistry of their Neutral Analogs. A Fourier-Transform Ion Cyclotron Resonance Study

Maurizio Speranza

Dipartimento di Studi di Chimica e Tecnologia delle Sostanze Biologicamente Attive, Università degli Studi di Roma "La Sapienza", P. le A. Moro 5, 00185 Rome, Italy

Received May 16, 1996[⊗]

The kinetics and the reaction patterns of the HO_3^+ and $H_2O_3^+$ ions toward a variety of inorganic and organic substrates have been investigated by using Fourier-transform ion cyclotron resonance (FT-ICR) spectrometry. The thermochemistry of the HO_3^+ and $H_2O_3^+$ ions is evaluated from correlations between their proton transfer (PT) efficiencies and the proton affinity (PA) of the selected substrates. Similarly, thermochemical data on HO_3 and H_2O_3 species are inferred from a comparison between the electron transfer (ET) efficiencies of their cationic counterparts and the standard ionization energies (IE) of the substrates. Thus, in striking contrast with most literature theoretical and empirical estimates, an experimental value of -1 ± 5 kcal mol^{-1} is obtained for the standard heat of formation of HO_3. Accordingly, ground-state HO_3 (^{2}A) is thermochemically stable toward dissociation to HO($^2\Pi$) and $O_2(^3\Sigma_g^-)$, and therefore, its existence as a true intermediate in key ionic reactions occurring in the upper atmosphere cannot be excluded. The standard formation enthalpy of $H_2O_3^+$ (198 ± 5 kcal mol^{-1}) is evaluated by two independent approaches, while that of the HOOOH neutral molecule is estimated as ≤ -26 kcal mol^{-1}. The HO_3^+ ion displays a variegated chemistry. Depending of the nature of the reactive centers of the neutral substrate, the HO_3^+ ion may react as a Brønsted or a Lewis acid, as an oxenium ion or an oxygen-centered free radical. When all these pathways are thermochemically precluded, as with CO, a ligand swiching process takes place in HO_3^+ to give the CHO_2^+ ion, which may promote a three-step acid-catalyzed cycle for the O_3 oxidation of CO to CO_2 and O_2. Likewise, the less reactive $H_2O_3^+$ ion undergoes ligand swiching by water.

Introduction

Ozone and hydrogen polyoxides are important species involved in chemical kinetics and equilibria of Earth's troposphere, stratosphere, and lower ionosphere, as well as key intermediates in research and industrial processes. The physics and chemistry of these species and of their ionic analogs have been the matter of intense investigation over the last 2 decades,[1−4] whose issues however have been often controversial. This situation arises from the peculiar electronic properties of ozone and of its neutral and ionic derivatives, which confer to them the character of extremely reactive and elusive species. Even the assignment of the electronic states of O_3 is far from complete and still in partial contradiction with most refined *ab initio* calculations.[5] This is due to the well-known difficulty in describing adequately the biradical character of the ground-state ozone,[6] which becomes entangled with other aspects of the electron correlation problem. For the same reasons, the theoretical description of the closed-shell hydrogen trioxide, H_2O_3, and of the open-shell hydrotrioxide, HO_3, is far from trivial and quite dependent upon the specific level of theory adopted (Table 1).[7−21]

Hydrogen trioxide, HOOOH, is a reactive intermediate long postulated in atmospheric and combustion chemistry,[18,27] as well as in chemical and biological oxidations.[28] While no H_2O_3 isomers have been detected in the gas phase, a species with the HOOOH structure has been generated and spectroscopically characterized in the condensed phase.[29−34] Hydrogen trioxide, HOOOH, has been the subject of several theoretical studies,

⊗ Abstract published in *Advance ACS Abstracts,* September 15, 1996.

(1) Steinfeld, J. I.; Alder-Golden, S. M.; Gallagher, J. W.*J. Phys. Chem. Ref. Data* **1987**, *16*, 911.
(2) Horvath, M.; Bilitzky, L.; Huttner, J. In *Topics in Inorganic Chemistry*; Clark, R. J. H., Ed.; 1985; Vol 20.
(3) Salem, L. *Electrons in Chemical Reactions: First Principles*; Wiley: New York, 1982.
(4) Plesnicar, B. *Organic Peroxides*; Ando, W., Ed.; Wiley: New York, 1992.
(5) Arnold, D. W.; Xu, C.; Kim, E. H.; Neumark, D. M. *J. Chem. Phys.* **1994**, *101*, 912.
(6) Goddard, W. A., III; Dunning, T. H., Jr.; Hunt, W. J.; Hay, P. J. *Acc. Chem. Res.* **1973**, *6*, 368.
(7) Benson, S. W. *Thermochemical Kinetics*; Wiley: New York, 1968.
(8) Blint, R. J.; Newton, M. D. *J. Chem. Phys.* **1973**, *59*, 6220.
(9) Nangia, P. S.; Benson, S. W. *J. Phys. Chem.* **1979**, *83*, 1138.
(10) Nangia, P. S.; Benson, S. W. *J. Am. Chem. Soc.* **1980**, *102*, 3105.
(11) Brich Mathisen, K; Gropen, O; Skancke, P. N.; Wahlgren, U. *Acta Chem. Scand. A* **1983**, *37*, 817.
(12) Brich Mathisen, K.; Sieghban, P. E. M. *Chem. Phys.* **1984**, *90*, 225.
(13) Dupuis, M.; Fitzgerald, G.; Hammond, B.; Lester, W. A., Jr.; Schaefer, H.F., III *J. Chem. Phys.* **1986**, *84*, 2691.
(14) Vincent, M. A.; Hillier, I. H.; Burton, N. A. *Chem. Phys. Lett.* **1995**, *233*, 111.
(15) Benson, S. W. *J. Chem. Phys.* **1960**, *33*, 306.
(16) Radom, L.; Hehre, W. J.; Pople, J. A. *J. Am. Chem. Soc.* **1971**, *93*, 289.
(17) Jackels, C. F.; Phillips, D. H. *J. Chem. Phys.* **1986**, *84*, 5013.
(18) Gonzales, C.; Theisen, J.; Zhu, L.; Schlegel, H. B.; Hase, W. L.; Kaiser, E. W. *J. Phys. Chem.* **1991**, *95*, 6784.
(19) Zhao, M.; Gimarc, B. *J. Phys. Chem.* **1993**, *97*, 4023.
(20) Vincent, M. A.; Hillier, I. H. *J. Phys. Chem.* **1995**, *99*, 3109.
(21) Koller, J.; Plesnicar, B. *J. Am. Chem. Soc.* **1996**, *118*, 2470.
(22) Kausch, M.; Schleyer, P.v.R. *J. Comput. Chem.* **1980**, *1*, 94.
(23) Meredith, C.; Quelch, G. E.; Schaefer, H. F., III *J. Am. Chem. Soc.* **1991**, *113*, 1186.
(24) Zakharov, I. I; Kolbasina, O. I.; Semenyuk, T. N.; Tyupalo, N.; Zhidomirov, G. M. *Zh. Strukt. Khim.* **1993**, *34*, 28.
(25) Cacace, F.; Speranza, M. *Science* **1994**, *265*, 208.
(26) Smith, G. P.; Lee, L. C. *J. Chem. Phys.* **1978**, *69*, 5393 and references therein.
(27) Gromov, A. R.; Antipenko, E. E.; Strakhov, B. V. *Zh. Fiz. Khim.* **1990**, *64*, 77.
(28) Cerkovnik, J.; Plesnicar, B. *J. Am. Chem. Soc.* **1993**, *115*, 12169.
(29) Czapski, G.; Bielski, B. H. J. *J. Phys. Chem.* **1963**, *67*, 2180.
(30) Bielski, B. H. J.; Schwarz, H. A. *J. Phys. Chem.* **1968**, *72*, 3836.
(31) Giguère, P. A.; Herman, K. *Can. J. Chem.* **1970**, *48*, 3473.

S0020-1669(96)00549-6 CCC: $12.00

Table 1. Literature Values of the Heats of Formation of Neutral and Cationic Hydrogen Trioxides

species	$H°_f$ (kcal mol^{-1})[a]	method	ref. no.	year
HO_3	−1.9 to +2.2	empiric	7	1968
	+23	RHF/4-31G	8	1973
	+21.8	empiric	9	1979
	+17.8	empiric	10	1980
	+27.3	RHF/4-31G	11	1983
	+10.7	CAS SFC	12	1984
	+12.7	CCI	12	1984
	−3.1	MCHF/DZP	13	1986
	+11.4	BD(T)/6-31G**	14	1995
	−13.1	B-LYP/6-31G**	14	1995
H_2O_3	−7	empiric	15	1960
	−16.7	LCAO/6-31G	16	1971
	−15	RHF/4-31G	8	1973
	−15.7	empiric	9	1979
	−17.7	empiric	10	1980
	−13.0	CI(SDQ)	17	1986
	+29.9	HF/6-31G**	18	1991
	−34.1	MP2/6-31G**	18	1991
	−20.1	MP3/6-31G**	18	1991
	−24.8	MP4/6-31G**	18	1991
	−15	RHF/6-31G**	19	1993
	−18	MP2/6-31G**	19	1993
	−17.8	QCISD/6-311++G(2d,p)	20	195
	−22.6	MP2/6-31G++G*	21	1996
	−26.0	MP4//MP2/6-31++CG*	21	1996
HO_3^+	+274	MP2/6-31G*	22	1980
	+250	CCSDT-CCSD	21	1991
	+241	MP4/4-31G	24	1993
	+252	bracketing (FT-ICR)	25	1994
$H_2O_3^+$	ca.+204	photodissociation	26	1978

[a] Figures in italics refer to approximated values calculated from isodesmic reactions at 0 K with no zero-point corrections.

which have highlighted the need for including electron correlation to predict the correct structure and energy (Table 1).[17,19,20,21,35]

The existence of hydrotrioxide radicals, HO_3, in the upper atmosphere has been hypothesized from time to time. Among others, the HO_3 radical has been suggested as a possible sink for O_2 ($^3\Sigma_g^-$, $^1\Delta_g$, $^3\Sigma_g^+$) and OH ($^2\Pi$), but, so far, no proofs of its existence have been collected.[36] Characterization of HO_3 as a local minimum on the potential energy surface relies exclusively upon theoretical calculations.[8,11−14,20] The results depend dramatically on the theoretical approach used (Table 1). Inclusion of electron correlation is recognized to be crucial for a correct description of the geometry and the electronic configuration of the HO_3 radical.[12] Nevertheless, recent application of the Brueckner doubles (BD) method and of the density functional theory (DFT) of treating electron correlation lead to largely different predictions of HO_3 as a sink of O_2 ($^3\Sigma_g^-$, $^1\Delta_g$, $^3\Sigma_g^+$) and OH ($^2\Pi$).[20] At the BD(T) level, HO_3 is predicted to be ca. 0.7 kcal mol^{-1} less stable than the O_2 ($^3\Sigma_g^-$) and OH ($^2\Pi$) products, whereas at the DFT level HO_3 is predicted to be more stable than O_2 ($^3\Sigma_g^-$) and OH ($^2\Pi$) by over 17 kcal mol^{-1}. However, all these theoretical studies consistently assign the open-chain HOOO structure, with the unpaired electron at the terminal oxygen, to the most stable HO_3 isomer.[14,20]

Comparatively few studies of the cationic analogs of hydrogen trioxide, i.e. $H_2O_3^+$, and of hydrotrioxide, i.e. HO_3^+, have appeared thus far. Olah and co-workers first proposed the intermediacy of HO_3^+ in superacid-catalyzed oxidation of alkanes with ozone.[37,38] However, attempts to observe HO_3^+ directly by ^{1}H-NMR spectroscopy were unsuccessful. Theoretical methods have been used to establish the existence, the structure, and the relative stability of isomeric HO_3^+ ions. Again, the results depend considerably on the theoretical approach and the basis set used,[22−24] although all these studies agree in assigning a terminally protonated, open-chain structure to the most stable form of HO_3^+, with a heat of formation ranging from 241 to 274 kcal mol^{-1} (Table 1). Only very recently, the elusive HO_3^+ intermediate has been generated in the source of a Fourier-transform ion cyclotron resonance (FT-ICR) spectrometer by protonation of ozone and its actual heat of formation (252 ± 3 kcal mol^{-1}) experimentally determined.[25] No information is hovewer available thus far about its chemistry in the gaseous phase.

The $H_2O_3^+$ ion is abundant in the lower ionosphere in the form of a weakly-bound adduct between O_2^+ and H_2O, i.e. $[H_2O{\cdot}O_2]^+$.[39,40] Important loss mechanisms of this ion from the lower ionosphere involve either visible sunlight photodissociation ($D°([H_2O{\cdot}O_2]^+) \geq 0.7$ eV, corresponding to $\Delta H°_f([H_2O{\cdot}O_2]^+) \leq 204$ kcal mol^{-1}; Table 1)[41,42] or proton transfer to water, with formation of either $[HO{\cdot}OH_3]^+$ (and O_2) or H_3O^+ (and O_2 + OH or, if actually accessible, HOOO).[39,40,43] Formation of $[HO{\cdot}OH_3]^+$ is thought to involve ground-state $[H_2O{\cdot}O_2]^+$. In contrast, the competing process leading to H_3O^+ may involve vibrationally excited $[H_2O{\cdot}O_2]^+$ ions, depending upon whether HOOO is actually formed (Table 1). No further information about the $[H_2O{\cdot}O_2]^+$ chemistry is presently available.

Neither experimental data nor theoretical predictions are even available about the actual existence and reactivity of another important $H_2O_3^+$ isomer, i.e. $HOOOH^+$, the cationic analog of hydrogen trioxide, HOOOH.

This paper represents a further contribution to the characterization of hydrogen trioxides and their cationic analogs, based upon the FT-ICR kinetic methodology already adopted in the identification of the elusive HO_3^+ intermediate.[25] The study has been performed by generating the HO_3^+ and $H_2O_3^+$ ions in the external source of the instrument by several ion-molecule reactions, using O_3 as the precursor. The HO_3^+ and $H_2O_3^+$ ions were allowed to react with a variety of organic and inorganic substrates, kept in the FT-ICR cell at defined concentrations. From the kinetic and mechanistic evaluation of the corresponding reaction patterns, it is hoped to provide more information about the structure and the stability of the HO_3^+ and $H_2O_3^+$ ions as well as about the actual existence and thermochemistry of their neutral analogs.

Experimental Section

Materials. Ozone was produced using a Fischer 502 ozonizer, which generates a silent electric discharge in a flow of dry oxygen.[2,44] The ozonized gas leaving the discharge contains only a few percent of ozone, but trapping the ozone at 195 K and washing away the excess oxygen with dry N_2 allows a gaseous O_3/N_2 mixture with a sufficiently high

(32) Deglise, X.; Giguère, P. A. *Can. J. Chem.* **1971**, *49*, 2242.
(33) Arnau, J. L.; Giguère, P. A. *J. Chem. Phys.* **1974**, *60*, 270.
(34) Yagodovskaya, T. V.; Zhogin, D. Y.; Nekrasov, L. I. *Zh. Fiz. Khim.* **1976**, *50*, 2736.
(35) Blahous, C. P., III; Schaefer, H. F., III *J. Phys. Chem.* **1988**, *92*, 959.
(36) Fehsenfeld, F. C.; Moseman, M.; Ferguson, E. E. *J. Chem. Phys.* **1971**, *55*, 2115.
(37) Olah, G. A.; Yoneda, N.; Parker, D. G. *J. Am. Chem. Soc.* **1976**, *98*, 5261.
(38) Yoneda, N.; Olah, G. A. *J. Am. Chem. Soc.* **1977**, *99*, 3113.
(39) Fehsenfeld, F. C.; Ferguson, E. E. *J. Geophys. Res.* **1969**, *74*, 2217.
(40) Ferguson, E. E.; Fehsenfeld, F. C. *J. Geophys. Res.* **1969**, *74*, 5743.
(41) Adams, N. G.; Bohme, D. K.; Dunkin, D. B.; Fehsenfeld, F. C.; Ferguson, E. E. *J. Chem. Phys.* **1970**, *52*, 3133.
(42) Howard, C. J.; Bierbaum, V. M.; Rundle, H. W.; Kaufman, F. *J. Chem. Phys.* **1972**, *57*, 3491.
(43) Good, A.; Durden, D. A.; Kebarle, P. *Proceedings of the Symposium of the Physics and Chemistry of the Upper Atmosphere*; Stanford Research Inst.: Palo Alto, CA, 24−25 June 1969.
(44) Mehandjiev, D.; Naidenov, A. *Ozone Sci. Eng.* **1983**, *14*, 277.

mole fraction of ozone to be prepared. Such a mixture was allowed to reach the room temperature in a 0.5-L bulb, suitably protected against explosions, and then directly connected to the inlet line of the external source of the FT-ICR instrument. Introduction of the ozone mixture into the instrument proved difficult in that ozone is an extremely reactive molecule, which rapidly decomposes when in contact with many metallic and non-metallic surfaces.[2,44] Hence, any sample of ozone introduced into the source of the mass spectrometer may easily be degraded, and a mixture of O_3 and O_2 in the source will result. Previous experimental studies indicate that this *in situ* degradation may exceed 10% of the O_3 present.[45] Most of the other chemicals used in the present study were commercially available and used without further purification. Hydrazoic acid, HN_3, was prepared from sodium azide and stearic acid and purified by repeated bulb-to-bulb distillation in a greaseless vacuum line.

Procedure. The experiments were performed using an APEX 47e FT-ICR mass spectrometer (Bruker Spectrospin). The primary O_3^+ ions were generated by 70-eV electron bombardment of a $N_2/O_3/O_2$ mixture introduced into the external source of the FT-ICR at room temperature and at nominal pressures from 8×10^{-6} to 1.2×10^{-5} Torr. Formation of O_5^+ ions was observed as well, in relative yields increasing with the source pressure.

When appropriate hydrogen donors, such as H_2 or CH_4 (8×10^{-5} Torr), are added to the $N_2/O_3/O_2$ mixture (9×10^{-6} Torr), the O_3^+ ions are partially converted into HO_3^+. With CH_4, minor amounts of $H_2O_3^+$ are formed as well.

In most kinetic experiments, the total pressure in the external FT-ICR source was normally around 8×10^{-6} to 1×10^{-4} Torr, as measured with an uncalibrated ionization gauge placed in a side arm of the main pumping line. The measure of the much lower pressures of the neutral reagents placed in the FT-ICR cell necessitates the use of an ion gauge whose sensitivity is dependent on the nature of the chemical species. The correction of the ionization gauge reading is achieved by first determining the rate constant for the reaction between the CH_4^+ radical cation and CH_4 with the FT-ICR instrument and then by comparing the obtained result with the average value of reported rate constants for this process (1.13×10^{-9} cm^3 molecule^{-1} s^{-1}).[46,47] Subsequently, the correction factor needed for other compounds may be estimated with the method based on an indicated linear dependence of the response of the ionization gauge with the polarizability of the neutral reagent in question.[48]

The ionic plasma, generated in the external FT-ICR source, was introduced in the FT-ICR cell containing a large excess of the appropriate reagent and, then, translationally and vibrationally quenched by collisions with Ar atoms pulsed into the cell through a magnetic valve. The desired starting ions, either HO_3^+ or $H_2O_3^+$, were then isolated by broad-band ejection and by "single shots"[49] and allowed to react with the appropriate neutral substrate. If thermal reactants are involved, all the reactions obey a pseudo-first-order kinetics since the number of ions is roughly a factor of 10^4 lower than of the neutral substrate in the FT-ICR cell. Indeed, in all systems investigated, an inverse linear dependence is observed between the natural logarithm of the relative abundance of the starting ionic species and the reaction time, with regression analysis correlation coefficients exceeding 0.990. Thence, the second-order rate constants (k_{obs}) are derived as the ratio between the slope of linear plots and the pressure of the substrate. The major uncertainties in the conversion of the pseudo-first-order rate constants to the second-order ones resides in establishing the pressure and the temperature of the gaseous substrate, taken as that of the inlet lines and of the main vacuum system (298 K). After the above corrections for the ion gauge readings, the experimental k_{obs} values are found to be reproducible within ca. 20%. Comparison of the k_{obs} values with the corresponding collision rate constants (k_{coll}), estimated according to the trajectory calculation method,[50] provides directly the efficiency of the reaction (eff $= k_{obs}/k_{coll}$). Phenomenological kinetic isotope effects were taken as the rate constant ratios of the reactions involving isotopomeric reactants (k_H/k_D) and found to be reproducible within ca. 30%.

Structural analysis of the HO_3^+ and $H_2O_3^+$ ions was performed by collision-induced dissociation (CID) experiments, carried out in the FT-ICR cell using Ar as the collision gas at ca. 1×10^{-7} Torr. The ions were accelerated by using an excitation pulse with a fixed amplitude ($2V_{p-p}$) and a variable duration (0.01−0.06 ms). With variation of the duration of the excitation pulse, dissociation products were measured for different estimated laboratory kinetic energies (10−220 eV), corresponding to center-of-mass energies ranging from 4 to 96 eV.

Results

Thermochemical calculations point to reactions 1 and 2 as the only energetically allowed routes to HO_3^+ ions (H = H or D) from 70-eV electron impact on $N_2/O_3/O_2$ mixtures, containing an excess of N_2 in the presence of the hydrogen donor H_2. The same ions may arise in the $CH_4/N_2/O_3/O_2$ plasma (H = H or D) from at least three exothermic channels, involving respectively the protonation of O_3 by CH_4^+ and CH_5^+ ions ($\Delta H° = -18$ kcal mol^{-1}) and the H-atom abstraction from CH_4 by O_3^+ ($\Delta H° = -16$ kcal mol^{-1}; eq 3).

$$O_3^+ + H_2 \rightarrow HO_3^+ + H \qquad \Delta H° = -17 \text{ kcal mol}^{-1} \quad (1)$$

$$N_2H^+ + O_3 \rightarrow HO_3^+ + N_2 \qquad \Delta H° = -31 \text{ kcal mol}^{-1} \quad (2)$$

The efficiency of reaction 3 was actually experimentally evaluated by generating O_3^+ in the external FT-ICR source and by measuring its reaction rate with CH_4, contained in the FT-ICR cell at 3×10^{-8} Torr. Abstraction of a H atom from CH_4 by O_3^+ is quite inefficient (eff $= k_{obs}/k_{coll} = 0.06 \pm 0.01$) and displays an appreciable isotope effect ($k_H/k_D = 1.5 \pm 0.3$).

$$O_3^+ + CH_4 \rightarrow HO_3^+ + CH_3; \Delta H° = -16 \text{ kcal mol}^{-1} \quad (3)$$

Collision-induced dissociations were used to characterize the HO_3^+ ions generated in the $H_2/N_2/O_3/O_2$ and $CH_4/N_2/O_3/O_2$ plasmas. In both systems, the isolated HO_3^+ ion loses exclusively the O_2^+ fragment (Figure 1a).

As mentioned before, small amounts of the $H_2O_3^+$ ions (H = H or D) accompany formation of HO_3^+ in the $CH_4/N_2/O_3/O_2$ plasma. Their origin was ascertained by investigating the reaction of HO_3^+ ions with CH_4 (3×10^{-8} Torr) in the FT-ICR cell. The HO_3^+ ions slowly abstract a hydrogen from CH_4 yielding HHO_3^+ ((a) in Table 2). The same reaction was observed by using HN_3 as the hydrogen donor, instead of CH_4 ((r) in Table 2). A further convenient way to produce $H_2O_3^+$ is based on the tendency of the O_5^+ ions, generated from 70-eV electron bombardment of the $N_2/O_3/O_2$ mixture in the external source of the FT-ICR by reaction 4,[51] to undergo substitution by H_2O ($k_{obs} = 9.8 \times 10^{-10}$ cm^3 molecule^{-1} s^{-1}, using $H_2{}^{18}O$ as substrate),[52] contained in the FT-ICR cell at 2×10^{-8} Torr pressure (eq 5).

$$O_3^+ + O_3 \rightarrow O_5^+ + O \quad (4)$$

$$O_5^+ + H_2O \rightarrow H_2O_3^+ + O_3 \quad (5)$$

The product patterns from the attack of the HO_3^+ and the $H_2O_3^+$ ions (H = H or D) on some representative substrates

(45) Johnstone, W. M.; Mason, N. J.; Newell, W. R.; Biggs, P.; Martson, G.; Wayne, R.P. *J. Phys. B* **1992**, *25*, 3873.
(46) Olmstead, W. N.; Brauman, J. I. *J. Am. Chem. Soc.* **1977**, *99*, 4219.
(47) Ikezoe, Y.; Matsuoka, S.; Takebe, M.; Viggiano, A. A. *Gas Phase Ion-Molecule Reaction Rate Constants Through 1986*; Maruzen Company, Ltd.: Tokyo, 1987.
(48) Bartmess, J. E.; Georgiadis, R. M. *Vacuum* **1983**, *33*, 149.
(49) De Koning, L. J.; Fokkens, R. H.; Pinkse, F. A.; Nibbering, N. M. M. *Int. J. Mass Spectrom. Ion Processes* **1987**, *77*, 95.
(50) Su, T.; Chesnavich, W. J. *J. Chem. Phys.* **1982**, *76*, 5183.
(51) Weiss, M. J.; Berkowitz, J.; Appleman, E. H. *J. Chem. Phys.* **1977**, *66*, 2049.
(52) Dotan *et al.* (Dotan, I.; Davidson, J. A.; Fehsenfeld, F. C.; Albritton, D. L. *J. Geophys. Res.* **1978**, *83*, 5414) report a $k = 1.2 \times 10^{-9}$ cm^3 molecule^{-1} s^{-1} for the same rection with H_2O, instead of $H_2{}^{18}O$.

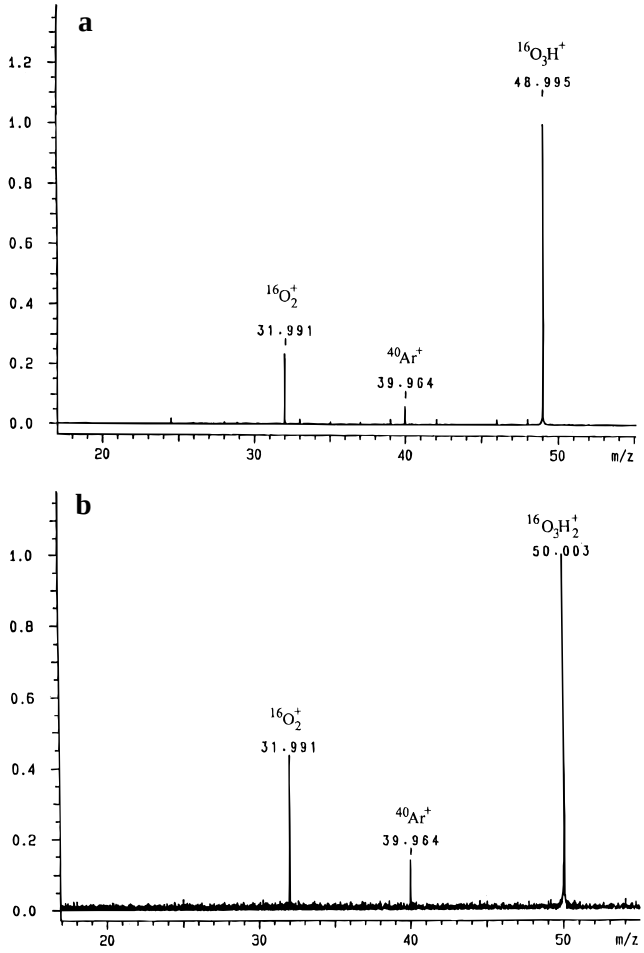

Figure 1. CID spectra of (a) $H^{16}O_3^+$ (m/z = 48.995) and (b) $H_2{}^{16}O_3^+$ (m/z =50.003), using Ar as target gas. The ion at m/z = 31.991 ($^{16}O_2^+$) corresponds to loss of $H^{16}O$ and $H_2{}^{16}O$, respectively. The peak at m/z = 39.964 ($^{40}Ar^+$) arises from high-energy charge transfer to the target gas.

are reported in Tables 2 and 3, respectively. The neutral species formed in these reactions are not detected with the present experimental method and only the elemental compositions of the expected neutral products are given in the equations of Tables 2 and 3.

Most substrates tend to release either an electron or a hydride ion to HO_3^+ and $H_2O_3^+$. For instance, propane reacts with HO_3^+ yielding exclusively $C_3H_8^+$ and $C_3H_7^+$ ((c) in Table 2). In the presence of their neutral precursor, these ionic products start the corresponding reaction pattern already observed in related mass spectrometric investigations. For instance, the time dependence of the concentrations of the $C_2H_4^+$, $C_2H_3^+$, and $C_2H_2^+$ ions from the attack of HO_3^+ on ethylene ((d) in Table 2) is consistent with the classical ethylene ion pattern, with these species as the precursors of the $C_3H_3^+$, $C_3H_5^+$, $C_4H_5^+$, and $C_4H_7^+$ products.

For most systems, the simple analysis of the dependence of the ion abundances with the reaction time allows determination of the reaction sequence occurring in the FT-ICR cell. A typical case is illustrated in Figure 2, concerning the reaction of HO_3^+ with bulk CO ((m) in Table 2).

The reported solid lines represent the theoretical time dependence of the relative yields of products for two consecutive first-order reactions, with the first reaction slower than the second one. Coincidence of the experimental results with the theoretical curves indicates that formation of CHO^+ from HO_3^+ actually proceeds through the $HO_3^+ \rightarrow CHO_2^+ \rightarrow CHO^+$ sequence. Further confirmation of the specific reaction sequence

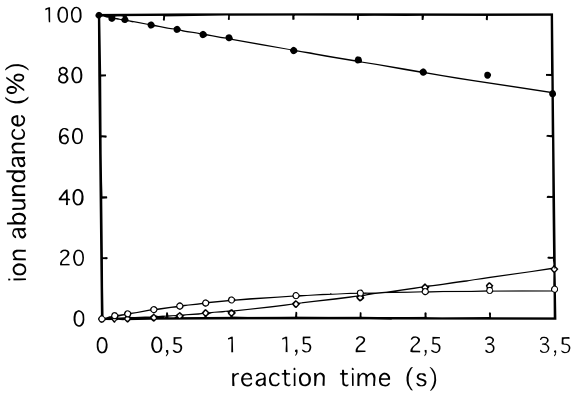

Figure 2. Time dependence of the abundances of the ionic products from attack of HO_3^+ on CO (3.4×10^{-8} Torr): HO_3^+ (full circles); CHO_2^+ (open circles); CHO^+ (diamonds). The solid lines describe the theoretical time dependence of the relative yields of products for two consecutive first-order reactions, with $k(HO_3^+ \rightarrow CHO_2^+) = 0.085$ s^{-1} and $k(CHO_2^+ \rightarrow CHO^+) = 0.7$ s^{-1}.

arises from multiple resonance experiments which allow isolation of the ion of interest (e.g. CHO_2^+) by applying appropriate frequency windows to remove all the undesired ions (i.e. HO_3^+) from the cell and by analyzing its progeny (i.e. CHO^+) after a suitable reaction time. Best fit of the experimental ion abundances with the theoretical curves provides the first-order rate constants of the individual steps ($k(HO_3^+ \rightarrow CHO_2^+) = 0.085$ s^{-1} and $k(CHO_2^+ \rightarrow CHO^+) = 0.7$ s^{-1}), which can be used to calculate the corresponding second-order values ($k(HO_3^+ \rightarrow CHO_2^+) = 1.0 \times 10^{-10}$ cm^3 molecule^{-1} s^{-1} and $k(CHO_2^+ \rightarrow CHO^+) = 8.5 \times 10^{-10}$ cm^3 molecule^{-1} s^{-1}), reported in Tables 2 (for HO_3^+) and 3 (for $H_2O_3^+$). The same procedures have been applied to all systems investigated. The rate constants of the first steps of the relevant reaction sequences are listed in Tables 2 and 3. The corresponding reaction efficiencies (eff = k_{obs}/k_{coll}) are listed in Tables 4 (for HO_3^+) and 5 (for $H_2O_3^+$).

Analysis of Table 4 reveals that substrates with the ionization enthalpies at 298 K (IE) exceeding 250.8 kcal mol^{-1} and proton affinities at 298 K (PA) ≤150 kcal mol^{-1}, namely CH_4, C_2H_6, C_3H_8, CO, and CH_3F, do not undergo extensive electron (ET) or proton transfer (PT) with the HO_3^+ ions. Instead, all these compounds (except, of course, CO) efficiently transfer a hydride ion (HT) to the ionic reactant. An appreciable kinetic isotope effect (k_H/k_D = 2.0 ± 0.3) is measured in the HT reaction between HO_3^+ and CH_4. CH_4 moieties are also able to transfer a H atom (HAT) to HO_3^+, yielding HHO_3^+ with no significant isotope effect (k_H/k_D=1.1 ± 0.2). A slow oxygen atom incorporation in all the members (except CH_3F) of this family of compounds is observed as well. In contrast, the HO_3^+ ions efficiently protonate substrates having IE ≥ 250.8 kcal mol^{-1}, but with PA > 150 kcal mol^{-1}, namely C_2H_2, $CH_2(CN)_2$, $H_2{}^{18}O$, and SO_2. Acetylene is able to incorporate one or two oxygen atoms as well. When interacting with HO_3^+, the substrates having IE ≤ 250.8 kcal mol^{-1}, but PA > 168 kcal mol^{-1}, namely allene (C_3H_4), fluorobenzene (C_6H_5F), H_2S, CH_2O, 1,1-difluoroethylene ($C_2H_2F_2$), and HN_3, undergo both extensive ET and PT reactions. The relative extent of the PT reaction appears to increase with the IE of the substrate, irrespective of its PA. Allene, H_2S, CH_2O, and HN_3, undergo the HT rection as well. Instead, both F^- or HF^- ions are formally transferred from 1,1-difluoroethylene to HO_3^+. Allene and 1,1-difluoroethylene undergo C−C bond fission as well, with concomitant incorporation of an oxygen atom. With C_2H_4 (IE = 242.3 kcal mol^{-1}; PA = 162.6 kcal mol^{-1}), the ET reaction with HO_3^+ is observed predominantly, together with pronounced H^- and H_2^- transfer and less extensive oxidation reactions.The ET reaction

Table 2. Product Patterns and Rate Constants (k_{obs}) of the Reactions of HO_3^+ (H = H, D) Ions with Neutral Substrates

substrate		products[a] H = H or D	relative yields (%) H = H	relative yields (%) H = D	k_{obs} ($\times 10^{10}$ cm^3 molecule^{-1} s^{-1})[b] H = H	k_{obs} ($\times 10^{10}$ cm^3 molecule^{-1} s^{-1})[b] H = D
(a) CH_4	→	$CH_3^+ + H\,HO_3$	67	68	1.28	1.25
	→	$CH_4^+ + HO_3$	24	23	0.45	0.41
	→	$CH_3O^+ + H\,HO_2$	7	7	0.14	0.13
	→	$H\,HO_3^+ + CH_3$	2	2	0.04	0.04
(a′) CD_4	→	$CD_3^+ + H_2O_3$	52		0.65	
	→	$CD_4^+ + HO_3$	37		0.46	
	→	$CD_3O^+ + HDO_2$	8		0.10	
	→	$H\,DO_3^+ + CD_3$	3		0.04	
(b) C_2H_6	→	$C_2H_5^+ + H\,HO_3$	69	69	3.76	3.80
	→	$CH_3O^+ + CH_3\,HO_2$	26	26	1.44	1.45
	→	$C_2H_5O^+ + H\,HO_2$	5	5	0.28	0.29
(c) C_3H_8	→	$C_3H_7^+ + H\,HO_3$	90	90	7.96	7.92
	→	$C_3H_8^+ + HO_3$	10	10	0.88	0.80
(d) C_2H_4	→	$C_2H_4^+ + HO_3$	45	46	4.45	4.45
	→	$C_2H_2^+ + H_2\,HO_3$	27	26	2.67	2.58
	→	$C_2H_3^+ + H\,HO_3$	22	22	2.18	2.17
	→	$C_2H_4O^+ + HO_2$	3	1	0.30	0.07
	→	$C_2H_3\,HO^+ + HO_2$		2		0.23
	→	$C_2H_3O^+ + H\,HO_2$	2	1	0.19	0.07
	→	$C_2H_2\,HO^+ + H_2O_2$		1		0.12
	→	$CH_2\,HO^+ + CH_2O_2$	1	1	0.05	0.05
(e) C_3H_6	→	$C_3H_6^+ + HO_3$	57	57	7.41	7.39
	→	$C_3H_5^+ + H\,HO_3$	34	21	4.42	2.71
	→	$C_3H_4\,H^+ + H_2O_3$		14		1.80
	→	$C_3H_3^+ + H_3\,HO_3$	9	8	1.17	1.10
(f) C_3H_4	→	$C_3H_4^+ + HO_3$	70	71	7.56	7.66
	→	$C_3H_4\,H^+ + O_3$	14	12	1.47	1.30
	→	$C_3H_3^+ + H\,HO_3$	13	14	1.46	1.55
	→	$C_2H_3\,HO^+ + CHO_2$	1	1	0.14	0.13
	→	$CH_2\,HO^+ + C_2H_2O_2$	2	2	0.20	0.22
(g) C_2H_2	→	$C_2H_2O^+ + HO_2$	48	55	2.33	2.29
	→	$C_2H_2\,H^+ + O_3$	38	28	1.82	1.19
	→	$C_2H_2O_2^+ + HO$	14	7	0.69	0.30
	→	$C_2H\,HO_2^+ + HO$		10		0.42
(h) CH_3F	→	$CH_2F^+ + H_2O_3$	75		3.07	
	→	$CH_4F^+ + O_3$	25		1.02	
(i) CCl_3F	→	$CCl_2F^+ + HClO_3$	77	77	2.19	2.19
	→	$CCl_3^+ + HFO_3$	20	20	0.57	0.57
	→	$CCl_3F^+ + HO_3$	3	3	0.08	0.08
(j) C_6H_5F	→	$C_6H_5F^+ + HO_3$	83	70	20.18	16.80
	→	$C_6H_4\,HF^+ + HO_3$		15		3.60
	→	$C_6H_5\,HF^+ + O_3$	17	15	4.13	3.55
(k) H_2S	→	$H_2S^+ + HO_3$	50	51	7.40	7.50
	→	$H_2\,HS^+ + O_3$	28	25	4.14	3.67
	→	$HS^+ + H\,HO_3$	22	24	3.26	3.53
(l) SO_2	→	$HSO_2^+ + O_3$	100	100	5.83	5.10
(m) CO	→	$C\,HO_2^+ + O_2$	100	100	1.04	1.06
(n′) $H_2{}^{18}O$	→	$H_3{}^{18}O^+ + O_3$	100		9.89	
(o) $CH_2(CN)_2$	→	$CH_2\,H(CN)_2^+ + O_3$	100	100	33.90	28.30
(p) CH_2O	→	$CH_2O^+ + HO_3$	45	52	11.31	12.10
	→	$CH_2\,HO^+ + O_3$	41	33	10.42	7.82
	→	$CHO^+ + H\,HO_3$	14	15	3.50	3.55
(q) $C_2H_2F_2$	→	$C_2H_2F_2^+ + HO_3$	63	64	9.45	9.51
	→	$C_2H_2F^+ + HFO_3$	17	17	2.52	2.50
	→	$CH_2F^+ + C\,HFO_3$	7	7	1.08	1.10
	→	$C_2H_2\,HF_2^+ + O_3$	6	5	0.91	0.65
	→	$C_2HF^+ + H\,HFO_3$	4	4	0.60	0.64
	→	$CH_2\,HO^+ + CF_2O_2$	3	3	0.51	0.48
(r) HN_3	→	$H\,HN_3^+ + O_3$	49	46	6.93	6.56
	→	$HN_3^+ + HO_3$	38	40	5.50	5.23
	→	$H\,HO_3^+ + N_3$	8	9	0.53	0.59
	→	$N_3^+ + H\,HO_3$	5	5	0.78	0.72

[a] The neutral species formed in these reactions are not detected with the present experimental method, and only the elemental compositions of the expected neutral products are given. [b] Uncertainty range: ca. 20%.

Table 3. Product Patterns and Rate constants (k_{obs}) of the Reactions of $H_2O_3^+$ (H = H, D) Ions with Neutral Substrates

substrate		products[a] H = H or D	relative yields (%) H = H	relative yields (%) H = D	k_{obs}($\times 10^{10}$ cm^3 molecule^{-1} s^{-1})[b] H = H	k_{obs}($\times 10^{10}$ cm^3 molecule^{-1} s^{-1})[b] H = D
(a) CH_4	→	no reaction				
(a′) CD_4	→	no reaction				
(b) C_2H_6	→	$C_2H_5^+ + H\ H_2O_3$	100	100	18.00	17.81
(d) C_2H_4	→	$C_2H_4^+ + H_2O_3$	82	82	10.37	10.12
	→	$C_2H_3^+ + H\ H_2O_3$	18	18	2.23	2.26
(k) H_2S	→	$H_2S^+ + H_2O_3$	73	77	13.90	13.84
	→	$H_2\ HS^+ + HO_3$	27	23	5.13	4.14
(l) SO_2	→	no reaction				
(m) CO	→	$C\ HO^+ + HO_3$	100	100	0.15	0.12
(n′) $H_2{}^{18}O$	→	$H_3{}^{18}O^+ + HO_3$	34		1.90	
	→	$H_4{}^{18}OO^+ + O_2$	34		1.90	
	→	$H_2{}^{18}O^+ + H_2O_3$	16		0.91	
	→	$H_2{}^{18}OO_2^+ + H_2O$	16		0.87	
(n″) D_2O	→	$HD_2O^+ + HO_3$	41		4.76	
	→	$H_2D_2O_2^+ + O_2$	30		3.41	
	→	$D_2O^+ + H_2O_3$	22		2.57	
	→	$D_2O_3^+ + H_2O$	7		0.83	
(o) $CH_2(CN)_2$	→	$CH_2\ H(CN)_2^+ + HO_3$	100	100	16.40	13.80
(p) CH_2O	→	$CH_2\ HO^+ + HO_3$	100	100	15.40	11.03
(r) HN_3	→	$HN_3^+ + H_2O_3$	72	76	8.70	8.54
	→	$H\ HN_3^+ + HO_3$	28	24	3.30	2.67
(s) CH_3OH	→	$CH_4\ HO^+ + HO_3$	34	31	6.80	5.84
	→	$CH_4O^+ + H_2O_3$	33	34	6.59	6.34
	→	$CH_3O^+ + H\ H_2O_3$	33	35	6.51	6.54
(t) CF_3CN	→	no reaction				
(u) PF_3	→	no reaction				

[a] The neutral species formed in these reactions are not detected with the present experimental method, and only the elemental compositions of the expected neutral products are given. [b] Uncertainty range: ca. 20%.

Table 4. Reaction Efficiencies in the Attack of HO_3^+ (H = H, D) Ions on Neutral Substrates[a]

substrate	PA (kcal mol^{-1})	IE (kcal mol^{-1})	PT[b]	ET	HT	others	total reacn efficiency
(a) CH_4	130.2	288.8	nd	0.043	0.123(1H)	0.004(*); 0.013(**)	0.183
(a′) CD_4	130.2	288.8	nd	0.043	0.062(1D)	0.003(***); 0.010(****)	0.118
(b) C_2H_6	142.7	265.7	nd	nd	0.327(1H)	0.024(*****); 0.125(**)	0.476
(c) C_3H_8	150	252.5	nd	0.070	0.632(1H)	nd	0.702
(d) C_2H_4	162.6	242.3	nd	0.377	0.184(1H); 0.226(2H)	0.018(#); 0.005(**); 0.028(§)	0.383
(e) C_3H_6	178.4	227.3	nd	0.617	0.368(1H); 0.097(3H)	nd	1.082
(f) C_3H_4	186	223.4	0.136	0.700	0.135(1H)	0.013(§); 0.018(**)	1.002
(g) C_2H_2	154	262.9	0.367	nd	nd	0.214(##); 0.063(§§)	0.644
(h) CH_3F	145	287.0	0.048	nd	0.144(1H)	nd	0.192
(i) CCl_3F	unknown	271.0	nd	nd	0.069(1F); 0.010(1Cl)	nd	0.079
(j) C_6H_5F	181.3	212.1	0.182	0.888	nd	nd	1.070
(k) H_2S	168.7	240.9	0.364	0.450	0.185(1H)	nd	0.999
(l) SO_2	150.9	283.9	0.360	nd	nd	nd	0.360
(m) CO	141.9	323.16	nd	nd	nd	0.129(###)	0.129
(n′) $H_2{}^{18}O$	165.0	250.8	0.417	nd	nd	nd	0.417
(o) $CH_2(CN)_2$	175.6	292.5	0.897	nd	nd	nd	0.897
(p) CH_2O	171.7	250.8	0.401	0.434	0.134(1H)	nd	0.969
(q) $C_2H_2F_2$	176	237	0.058	0.606	0.161(1F); 0.039(1HF)	0.033(**)	0.897
(r) HN_3	179	247.2	0.420	0.527	0.056(1H)	0.047(*)	1.050

[a] Uncertainty range: ca. 20%. Key: (*) $H\ HO_3^+$; (**) CH_3O^+; (***) $D\ HO_3^+$; (****) CD_3O^+; (*****) $C_2H_5O^+$; (#) $C_2H_3O^+$; (§) $C_2H_4O^+$; (##) $C_2H_2O^+$; (§§) $C_2H_2O_2^+$; (###) CHO_2^+. [b] Key: nd = below efficiency limit, ca. 0.001.

is observed with cyclopropane (C_3H_6) (IE = 227.3 kcal mol^{-1}; PA = 178.4 kcal mol^{-1}) as well, together with formal H^- and H_3^- transfers.

Similar reaction patterns are observed from the attack of the $H_2O_3^+$ ions on the same substrates (Table 5). Thus, compounds with IE ≥ 250.8 kcal mol^{-1} and PA ≤ 165 kcal mol^{-1} are either inert (CH_4, SO_2, CF_3CN, and PF_3) or poorly reactive (C_2H_6, CO, and water). Ethane slowly loses a hydride ion to $H_2O_3^+$. Water behaves in peculiar way since it is the only substrate able to formally accept an oxygen from $H_2O_3^+$. Substrates with IE ≥ 250.8 kcal mol^{-1} and PA > 165 kcal mol^{-1}, namely $CH_2(CN)_2$ and CH_2O, are exclusively and efficiently protonated by the $H_2O_3^+$ ions. Ethylene (IE = 242.3 kcal mol^{-1}; PA = 162.6 kcal mol^{-1}) undergoes efficient ET, accompanied by a less extensive HT reaction. The substrates with IE < 250.8 kcal mol^{-1} and PA > 165 kcal mol^{-1}, i.e. H_2S, HN_3, and CH_3OH, undergo both ET and PT reactions, with the relative extent of the PT reaction decreasing with the IE and the PA of the substrate. An important HT channel is observed in the reaction between $H_2O_3^+$ and CH_3OH as well.

Table 5. Reaction Efficiencies in the Attack of $H_2O_3^+$ (H = H, D) Ions on Neutral Substrates[a]

substrate	PA (kcal mol^{-1})	IE (kcal mol^{-1})	PT[b]	ET	others	total reacn efficiency
(a) CH_4	130.2	288.8	nd	nd	nd	
(a′) CD_4	130.2	288.8	nd	nd	nd	
(b) C_2H_6	142.7	265.6	nd	nd	0.158(*)	0.158
(d) C_2H_4	162.6	242.3	nd	0.910	0.196(**)	1.106
(k) H_2S	168.7	240.9	0.348	0.942	nd	1.290
(l) SO_2	150.9	283.9	nd	nd	nd	
(m) CO	141.9	323.16	0.019	nd	nd	0.019
(n′) $H_2{}^{18}O$	165.0	250.8	0.080	0.039	0.080(#); 0.037(##)	0.236
(n″) D_2O	165.0	250.8	0.202	0.109	0.144(§); 0.035(§§)	0.490
(o) $CH_2(CN)_2$	175.6	292.5	0.480	nd	nd	0.480
(r) HN_3	179	247.2	0.330	0.870	nd	1.200
(p) CH_2O	171.7	250.8	0.591	nd	nd	0.591
(s) CH_3OH	181.7	250.2	0.342	0.331	0.327(***)	1.000
(t) CF_3CN	159.3	319.4	nd	nd	nd	
(u) PF_3	162.5	264	nd	nd	nd	

[a] Uncertainty range: ca. 20%. Key: (*) $C_2H_5^+$; (**) $C_2H_3^+$; (#) $H_4{}^{18}OO^+$; (##) $H_2{}^{18}OO_2^+$; (§) $H_2D_2O_2^+$; (§§) $D_2O_3^+$; (***) CH_2OH^+. [b] Key: nd = below efficiency limit, ca. 0.001.

Discussion

The HO_3^+ and $H_2O_3^+$ (H = H or D) Reagents. The excellent agreement between the CCSDT-1/CCSD calculated protonation energy of ozone (148 kcal mol^{-1} at 0 K, corresponding to ca. 149.5 kcal mol^{-1} at 298 K)[23] and its proton affinity (PA = 148 ± 3 kcal mol^{-1} at 298 K), measured experimentally with the FT-ICR bracketing technique (Table 1),[25] shows that any description with quantitative accuracy of the intricate potential-energy hypersurface of protonated ozone HO_3^+ demands the use of highly sophisticated correlated methods with large basis set (the standard double-ζ plus polarization (DZ+P) set of Huzinaga and Dunning in ref 23) and reassures about the superior performance of these theoretical methods in reproducing simultaneously the geometry and the electronic properties of this species. The CCSDT-1/CCSD lowest energy form of HO_3^+ is the $[H-O(1)-O(2)-O(3)]^+$ planar one with the H−O(1) bond roughly perpendicular to the O(1)−O(2) bond axis and *trans* to the O(2)−O(3) one. In $[H-O(1)-O(2)-O(3)]^+$, the diradical configuration of its O3 (C_{2v}) precursor is partially destroyed. The electron density is redistributed over all the centers, mainly on the O(1) atom, as suggested by the location of a great deal of the positive charge at the H and O(3) ends. According to its structure and electronic configuration, the $[H-O(1)-O(2)-O(3)]^+$ ion may simultaneously have the character of a Brønsted (the H−O(1) proton) and of a Lewis acid (the O(3) center), as well as that of a radical- (the O(1) atom) and carbene-like species (the O(3) center). The open-chain [H−O−O−O] connectivity of the HO_3^+ ions from reactions 1−3 is consistent with results of its CID spectrum (Figure 1a). In view of the hardly accessible protonated O_3 (D_{3h}) structure (calculated 47.1 kcal mol^{-1} above the open chain form),[23] the exclusive loss of the HO fragment observed in the CID spectra of HO_3^+ conforms to its open-chain H−O−O−O$^+$ structure.

Sequence 4−5 represents one of the most convenient procedures to generate $H_2O_3^+$ (H = H or D) ions in the FT-ICR cell. The sequence involves the relatively abundant formation of O_5^+ ions (eq 4), which readily reacts with H_2O via eq 5. The product of this reaction is recognized as the $[H_2O{\cdot}O_2]^+$ adduct, which, in the upper atmosphere, undergoes subsequent attack by other water molecules, yielding eventually stable water cluster ions.[52] The CID spectrum of the $H_2O_3^+$ ion, obtained in the FT-ICR cell by reaction of O_5^+ with H_2O, conforms to the above structure, since it displays the exclusive loss of O_2^+ (Figure 1b).[53] Further support to this conclusion arises from the observation that, in the presence of $H_2{}^{18}O$, O_5^+ gives exclusively $[H_2{}^{18}O{\cdot}O_2]^+$, without any further label incorporation ((n′) in Table 3). This result, coupled with the predominant loss of $H_2{}^{18}O$ observed in the CID spectrum of the so-formed $[H_2{}^{18}O{\cdot}O_2]^+$, excludes the facile rearrangement of the $[H_2{}^{18}O{\cdot}O_2]^+$ structure into the $[H^{18}OOOH]^+$ one, which would allow rapid mixing of its terminal oxygens ($[H^{18}OOOH]^+ \rightarrow [H_2O{\cdot}{}^{18}O_2]^+$). Similar pieces of evidence were obtained for the HHO_3^+ ions, generated in the FT-ICR cell by hydrogen transfer from either CH_4 or HN_3 to HO_3^+, thus pointing to a [HH = O−O−O] connectivity.

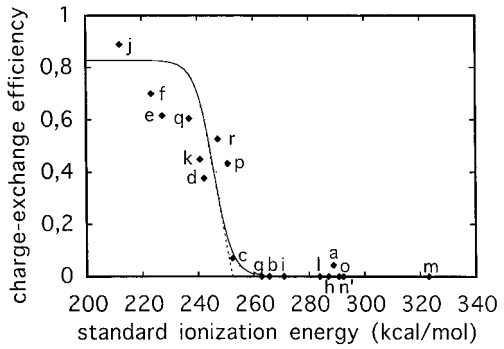

Figure 3. Electron transfer (ET) efficiency of HO_3^+ as a function of the standard ionization energy (IE) of neutral electron donors. Lettering is as in Tables 2 and 4.

Thermochemistry of HO_3^+ and $H_2O_3^+$ Ions and of Their Neutral Counterparts. Careful examination of the ET efficiencies between HO_3^+ and the selected substrates (Table 4) allows determination of the electron recombination enthalpy (RE) of the HO_3^+ ion at 298 K, which in turn provides an estimate of the standard heat of formation of the corresponding neutral, i.e. HO_3. When plotted against the ionization enthalpy at 298 K (IE) of the selected neutrals,[54,55] the ET efficiencies of Table 4 cluster along a sigmoid curve (Figure 3). A significant reaction efficiency is taken as an indication that ET from the reference neutrals to the HO_3^+ ion is energetically allowed, whereas a negligible efficiency is taken as evidence that the same process is energetically unfavored. Only within the hypothesis of encounter complexes between the neutral

(53) Susic, R.; Kralj, B.; Zigon, D. *Rapid Commun. Mass Spectrom.* **1995**, *9*, 64.
(54) Lias, S. G.; Bartmess, J. E.; Liebman, J. F.; Holmes, J. L.; Levin, R. D.; Mallard, W. G. *J. Phys. Chem. Ref. Data* **1988**, *17*, Suppl. No. 1.
(55) Szulejko, J. E.; McMahon, T. B. *J. Am. Chem. Soc.* **1993**, *115*, 7839.

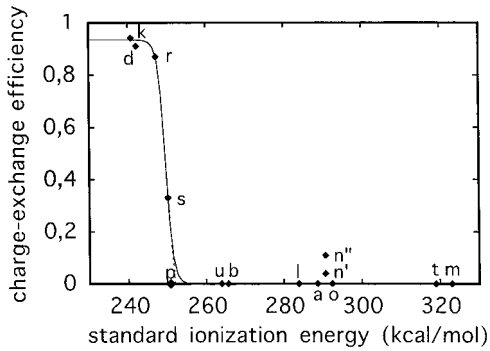

Figure 4. Electron transfer (ET) efficiency of $H_2O_3^+$ as a function of the standard ionization energy (IE) of neutral electron donors. Lettering is as in Tables 3 and 5.

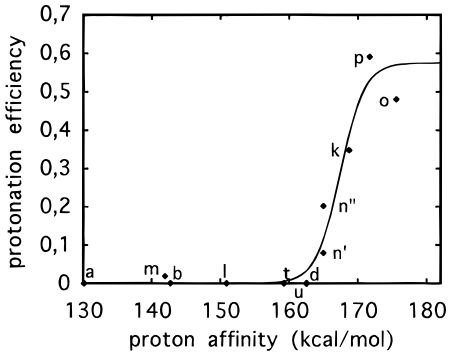

Figure 5. Proton transfer (PT) efficiency by $H_2O_3^+$ as a function of the proton affinity (PA) of neutral bases. Lettering is as in Tables 3 and 5 (for systems (r) and (s), see ref 59).

donors and the ionic acceptor sufficiently long lived to allow structural relaxation after the electron transfer, can the phenomenological RE of the HO_3^+ ion be identified as the IE of the corresponding neutral species HO_3. In this perspective, the IE of HO_3 would be taken as equal to the IE of the reference neutral corresponding to the inflection point of the sigmoid curve of Figure 3. However, electron transfer follows the Franck−Condon principle by taking place well before structural relaxation of the involved moieties. In this case, the actual IE of HO_3 would exceed the measured RE of the HO_3^+ ion by a quantity corresponding to the structural relaxation energies of both the donor and the acceptor. In this view, a better estimate of the IE of HO_3 at 298 K is provided by the onset of the sigmoid curve of Figure 3, corresponding to a value of 253 ± 4 kcal mol^{-1}.

On the basis of $H°_f(HO_3^+) = 252 \pm 3$ kcal mol^{-1},[25] the IE(HO_3) = 253 ± 4 kcal mol^{-1} leads to a standard formation enthalpy of HO_3 of −1 ± 5 kcal mol^{-1}, a value which is in substantial agreement with the MCHF/DZP theoretical predictions by Schaefer and co-workers (Table 1).[13] According to this value, ground-state HO_3 (^{2}A) is stable toward dissociation to HO($^2\Pi$) and $O_2(^3\Sigma_g^-)$ by at least 10 ± 5 kcal mol^{-1}, and therefore, in contrast with previous indications,[8,11,56] it may play a role as a true intermediate in key ionic reactions occurring in the atmosphere, such as $H(^2S)+O_3(^1A_1) \rightarrow HO_3(^2A) \rightarrow HO(^2\Pi) + O_2(^3\Sigma_g^-)$[13] and in the conversion of the $O_2^+ \cdot OH_2$ adduct to H_3O^+ clusters.[36,57,58] Work is in progress to independently confirm the existence of HO_3 as a stable species.

Figure 4 reports a plot of the ET reaction efficiencies between $[H_2O \cdot O_2]^+$ and the selected substrates (Table 5) as a function of their ionization enthalpy at 298 K (IE).[54,55] As for HO_3^+, the ET efficiencies of Table 5 fit a sigmoid curve, whose onset can be placed at 251 ± 3 kcal mol^{-1} and regarded as a reasonable estimate of the RE of the cation. In view of the dissociative character of the final state (either $H_2O + O_2(^1\Delta_g)$ or $H_2O + O_2(^3\Sigma_g^-)$[20]) of the electron attachment to $[H_2O \cdot O_2]^+$, the measured RE($[H_2O \cdot O_2]^+$) = 251 ± 3 kcal mol^{-1} provides an estimate of the lower limit of standard formation enthalpy of $[H_2O \cdot O_2]^+$, which amounts to ≥193 ± 3 kcal mol^{-1} (with $H_2O+O_2(^3\Sigma_g^-)$ as the dissociation products). The corresponding $[H_2O \cdot O_2]^+ \rightarrow H_2O+O_2^+$ dissociation energy (DE) is placed ≤27 ± 3 kcal mol^{-1}, a value which is consistent with the DE lower limit measured in flowing-afterglow experiments (≥16 kcal mol^{-1}).[39−41] Another experimental estimate of the standard formation enthalpy and DE of $[H_2O \cdot O_2]^+$ is obtained from the measurement of the PA of the HO_3 radical.

The gas-phase PA of HO_3 is measured with the well-established bracketing technique, which is based on the measurement of the efficiency of the proton transfer from the $[H_2O \cdot O_2]^+$ ion to a gaseous base of appropriate strength. For systems allowing exclusively or predominantly the proton transfer process, a high PT efficiency is taken as an indication that the PA of the reference base exceeds that of the cation, whereas a negligible PT efficiency is taken as evidence that the PA of the conjugate base of the cation (i.e. HO_3) exceeds that of the reference base. Strictly speaking, the latter inference is not rigorous, because a PT inefficiency could reflect the operation of kinetic, rather than thermodynamic, factors. This, however, seems unlikely in this case, because exothermic PT reactions that involve sterically unhindered n-type bases (e.g. CO, CF_3CN, or SO_2) are generally observed to occur at, or nearly at, the collision rate.[59] The results of the bracketing experiments are given in Figure 5. They refer to the protonation efficiency of $H_2O_3^+$ toward those reference bases exhibiting exclusive or predominant PT reaction.[60] Since timing of proton transfer between a donor and an acceptor is much longer than any electron transfer process, the PT encounter complex may be sufficiently long lived to allow complete structural relaxation of the involved moieties. In this case, a reasonable estimate of the PA of HO_3 can be inferred from the PA of the reference base corresponding to the inflection of the sigmoid curve interpolating the experimental results (PA(HO_3) = 167 ± 2 kcal mol^{-1} at 298 K). Taking $H°_f(HO_3) = -1 \pm 5$ kcal mol^{-1}, the PA(HO_3) = 167 ± 2 kcal mol^{-1} value leads to a standard formation enthalpy of $H_2O_3^+$ of 198 ± 5 kcal mol^{-1}, in agreement with the lower limit (≥193 ± 3 kcal mol^{-1}), inferred from the above RE($H_2O_3^+$) measurement (with $H_2O+O_2(^3\Sigma_g^-)$ as the dissociation products), and with the approximate value of ca. 204 kcal mol^{-1} derived from photodissociation experiments.[26] Taking 198 ± 5 kcal mol^{-1} as the standard formation enthalpy of $H_2O_3^+$, the DE($H_2O_3^+$) amounts to 22 ± 5 kcal mol^{-1}, a value which fits the linear correlation observed between the DE($B \cdot O_2^+$) values for several B molecules clustered to O_2^+, obtained by flowing-afterglow measurements of ligand exchange reactions (Figure 6)[41] and the PA of the ligand B (correlation coefficent = 0.983).

(56) Chen, M. M. L.; Wetmore, R. W.; Schaefer, H. F., III *J. Chem. Phys.* **1981**, *74*, 2938.
(57) Ferguson, E. E. In *Ion-Molecule Reactions*; Franklin, J. L. Ed.; Butterworths: London, 1972; Vol. 2, Chapter 8.
(58) Ferguson, E. E.; Fehsenfeld, F. C.; Albritton, D. L. In *Gas-Phase Ion Chemistry*; Bowers, M. T. Ed.; Academic Press: New York, 1979; Vol. 1, Chapter 2.
(59) The PT efficiency can be depressed if the PT process is nearly thermoneutral or if hindered bases are involved; cf.: Bucker, H.; Grutzmacher, H. F. *Int. J. Mass Spectrom. Ion Processes* **1991**, *109*, 95.
(60) The PT efficiencies from $H_2O_3^+$ to HN_3 ((r) in Table 5) and CH_3OH ((s) in Table 5) do not apparently fit the interpolating curve of Figure 5. This derives from the fact that, in these systems, the PT reaction undergoes competion from an efficient ET process and, therefore, the comparatively low PT efficiencies do not reflect a slow PT reaction, but just the branching ratio between two fast, competing processes.

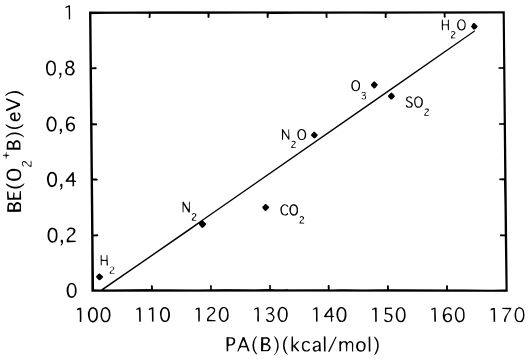

Figure 6. Linear correlation between the standard binding energy (BE) of $[O_2 \cdot B]^+$ and the proton affinity (PA) of molecule B.

Reactivity of the HO_3^+ (H = H or D) Ion. As mentioned in the Introduction, Olah and co-workers provided the first evidence of the occurrence of HO_3^+ in cold superacidic solutions containing ozone and of its tendency to insert into the σ-bonds of alkanes.[37] The evidence was based on the evaluation of the extent of alternative processes leading to the same oxidation products, one involving preliminar protolysis of the alkane followed by ozone quenching of the formed alkyl cation and the other proceeding through initial O_3-oxidation of the alkane to an alcohol followed by formation and O_3-quenching of the corresponding alkyl cation. In some systems, several of these oxidation mechanisms may be operative, whose relative extent is determined by many factors, including the nature of the alkane, the strength of the superacid, and the reaction temperature. Unequivocal discrimination among them is prevented by the difficulty in differentiating by NMR spectroscopy among the active precursors of the observed ionic products. In the present FT-ICR study, this difficulty is completely removed. Indeed, the HO_3^+ ion is formed in the external source of the instrument, i.e. completely away from the neutral substrate, and structurally characterized. The kinetics and the mechanism of its attack on the target molecule can be defined in the absence of perturbing solvation and ion-pairing phenomena, thus providing otherwise inaccessible information upon its intrinsic reactivity properties.

Saturated Hydrocarbons. Besides the ET reaction, ca. 67% of the reactive collisions between HO_3^+ and CH_4 (4×10^{-8} Torr) lead to the HT product CH_3^+, ca. 7% to the oxygenated CH_3O^+ fragment, and ca. 2% to the HAT derivative $H_2O_3^+$ (Table 4). Both CH_3O^+ and $H_2O_3^+$ products are relatively long lived in the reaction medium, whereas CH_3^+ rapidly disappears, yielding its $C_2H_5^+$ daughter by collision with the bulk CH_4. This, in turn, efficiently transfers a proton to water, invariably present in traces in the FT-ICR cell (ca. 10^{-9} Torr).

Similarly, HT and HAT reactions between DO_3^+ and CH_4 produce CH_3^+ and HDO_3^+, respectively, whereas oxygen incorporation yields CH_3O^+ predominantly (>80%), together with minor amounts of CDH_2O^+ (<20%). No appreciable deuterium effect is involved in the formation of these products from the CH_4/HO_3^+ (H = H or D) systems. No H-to-D exchange is detected in the DO_3^+ ions when they interact with CH_4.

When involving HO_3^+ and CD_4, the same processes lead to CD_3^+, HDO_3^+, and CD_3O^+ (>80%; CHD_2O^+ <20%). A direct deuterium effect is observed in the kinetics of the H^- transfer from CH_4 (H = H or D) to HO_3^+ ($k_H/k_D = 2.0 \pm 0.3$). Formation of CD_3O^+ displays a significantly lower kinetic isotope effect ($k_H/k_D = 1.3 \pm 0.2$), which becomes negligible in the formation of HHO_3^+ ($k_H/k_D = 1.1 \pm 0.2$). Again, no appreciable D-to-H exchange is observed in the HO_3^+ ions when they interact with CD_4.

Scheme 1

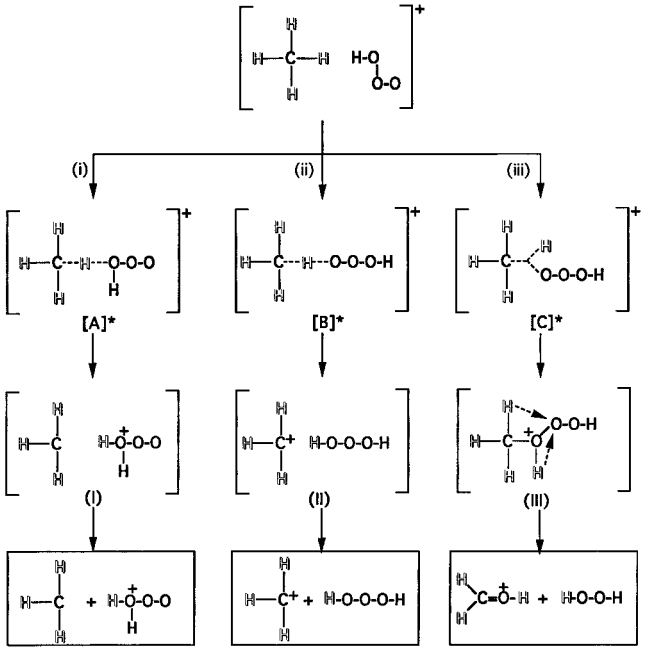

Indications about the most probable pathways operating in these systems can be drawn from thermodynamic and kinetic considerations, from the observed product distributions, and from the structural and electronic properties of the ionic reactant. Thus, the $[HHO \cdot O_2]^+$ structure arising from the quasi-thermoneutral HAT from CH_4 to HO_3^+ points to the O(1) atom of the ion, i.e. that with the greater spin density, as the predominant reaction center (eq i in Scheme 1). The reaction proceeds through the transition state $[\mathbf{A}]^‡$ involving a partial rupture of the C−H bond of the alkane. Subsequent fragmentation of adduct **I** produces a free CH_3 radical and the $[HHO \cdot O_2]^+$ ion. Formation of **I** is not reversible, as testified to by the lack of any detectable D(H) incorporation in HO_3^+ (DO_3^+) when it reacts with CD_4 (CH_4).

In principle, formation of the CH_3^+ fragment in the same systems can be accounted for by a rapid electron jump from the CH_3 radical to the HHO_3^+ moiety in adduct **I** (H = H or D) before its fragmentation. However, such a possibility is safely ruled out by the negligible deuterium effects, measured in the formation of $[HHO \cdot O_2]^+$ ($k_H/k_D = 1.1 \pm 0.2$), as compared to the appreciable one, observed in the formation of CH_3^+ ($k_H/k_D = 2.0 \pm 0.3$). This significant difference excludes that the processes leading to CH_3^+ and HHO_3^+ involve the same transition state, i.e. $[\mathbf{A}]^‡$. Besides, the absence of detectable deuterium effects in the formation of CH_3^+ from the attack of HO_3^+ on CH_4 speaks against a conceivable HT mechanism involving a $[H_3C \cdots H \cdots H \cdots O_3]^+$ transition state. Instead, the $k_H/k_D = 2.0 \pm 0.3$ isotope effects are consistent with a mechanism involving the hydride transfer from CH_4 to the O(3) atom of HO_3^+, namely the oxygen atom with the highest positive charge (eq ii in Scheme 1). The same mechanism accounts for the CH_4 oligomerization sequence observed by Olah and co-workers in "magic acid" (HSO_3F-SbF_5) cold solutions of O_3.[37] Accordingly, extensive occurrence of the HT channel ii of Scheme 1 is justified only if thermochemically allowed. This means that the $H_f°(HOOOH) \leq -26 \pm 3$ kcal mol^{-1}, a value which is consistent with the recent MP4//MP2/6-31++G** theoretical predictions by Koller and Plesnicar (Table 1).[21] Oxygen incorporation into CH_4 by HO_3^+ is a rather inefficient process (eff = 0.010−0.013) (Table 4), yielding exclusively a long-lived $[H_3, C, O]^+$ product. The complete absence of an accompanying CHO^+ fragment excludes that the long-lived $[H_3,$

Scheme 2

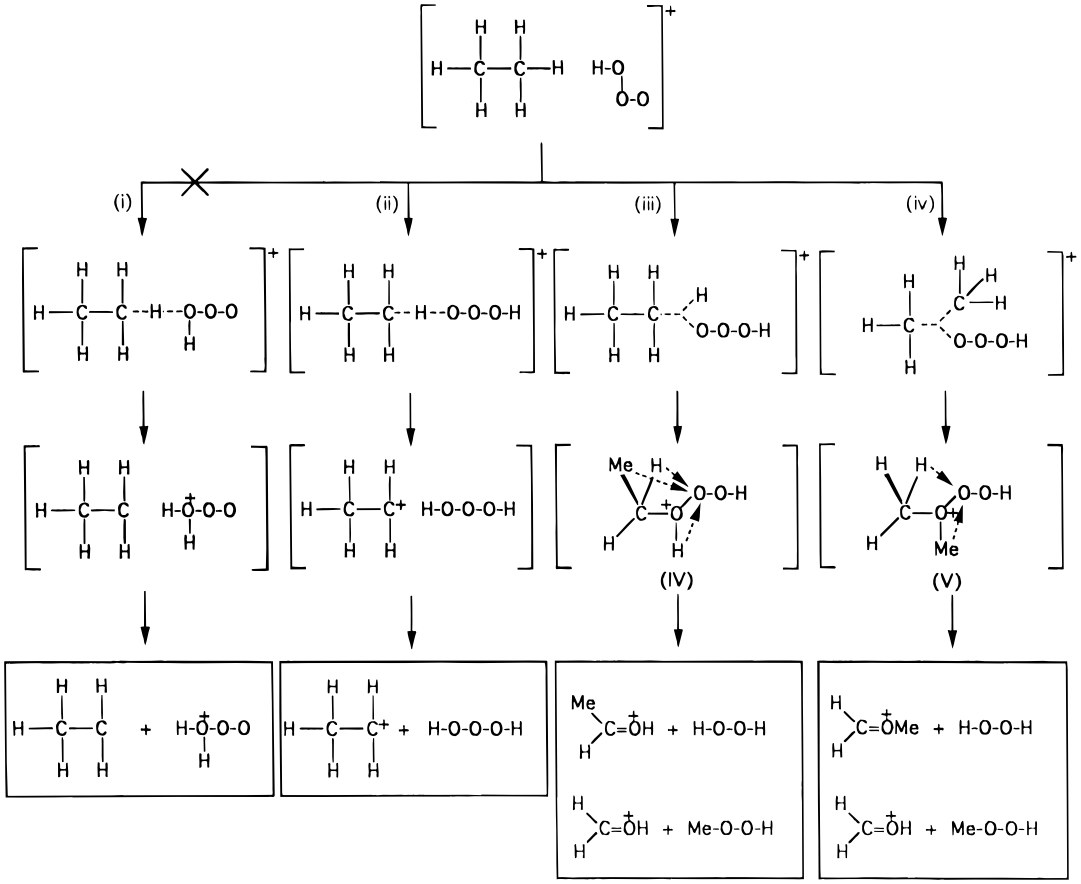

C, O]$^+$ product is the triplet methoxy cation CH_3O^+, which is known to partially fragment to H_2 and CHO^+.[61,62] Thus, the most likely structure of [H_3, C, O]$^+$ is that of the hydroxymethyl cation CH_2OH^+, which is unable to protonate water ($\Delta H° = +5$ kcal mol^{-1}).[54,55]

Given the oxenium ion character of the O(3) center of HO_3^+, the CH_2OH^+ product is thought to proceed from the insertion of HO_3^+ into a C−H bond of CH_4 via intermediate **III** (sequence iii of Scheme 1). A simple O(3)-to-O(2) H shift in **III** would promote the release of HHO_2 and the singlet CH_3O^+ cation, which immediately rearranges to CH_2OH^+.[61,62] Alternatively, **III** may first rearrange by a C-to-O(2) H shift and then fragment by releasing directly the CH_2OH^+ ion. Which of these two pathways governs formation of the CH_2OH^+ ion in the HO_3^+/CH_4 systems is still open to question. Similar mechanisms have been postulated by Olah and co-workers for the oxygen incorporation into some alkanes dissolved in cold solutions of "magic acid" (HSO_3F-SbF_5) containing O_3.[37,38]

Other conceivable mechanisms, such as the one involving recombination of the CH_3^+ ion with the HHO_3 moiety (or its HHO product)[18] in adduct **II** (sequence ii of Scheme 1) can be safely ruled out, since it involves the intermediacy of a vibrationally excited [CH_3OHH]$^+$ ion, which would readily 1,2-eliminate either a H_2 or a HH molecule.[63] Both CH_2OH^+ and CH_2OH^+ would be formed in comparable proportions, in contrast with the experimental findings ([CH_2OH^+]/[CH_2OD^+] = 4 from the DO_3^+/CH_4 systems; [CD_2OD^+]/[CD_2OH^+] = 4 from the HO_3^+/CD_4 systems). Refusal of this mechanistic hypothesis is further supported by the largely different deuterium effects observed in the formation of the CH_3^+ ($k_H/k_D = 2.0 \pm 0.3$) and the CH_2OH^+ fragment ($k_H/k_D = 1.3 \pm 0.2$) from HO_3^+ and CH_4 which exclude the occurrence of a common transition state, i.e. [**B**]‡.

In the ethane/HO_3^+ (H = H, D) systems, the HAT reaction i of Scheme 2 does not occur to any detectable extent. Rather, the HT process leading to $C_2H_5^+$ (68%) (path ii of Scheme 2) by far predominates over those yielding long-lived CH_2OH^+ (26%) and [H_5, C_2, O]$^+$ ions (5%) (Tables 2 and 4). The relative distribution of these oxygen-containing products strikingly contrasts with that observed in superacidic O_3/C_2H_6 solutions, where CH_2OH^+ is absent and protonated acetaldehyde $CH_3-CH{=}OH^+$ is the major product formed from insertion of HO_3^+ into a C−H bond of the alkane.[37] This apparent discrepancy can be rationalized by considering that, in the gas phase, HO_3^+ may readily insert into both the C−H and the C−C bonds of ethane yielding both **IV** and **V** intermediates (pathways iii and iv of Scheme 2), whereas formation of **V** is made more difficult in superacidic solutions by the bulkiness of the solvated ion-counterion pair.[37]

In the propane/HO_3^+ (H = H, D) systems, the major reaction channel is HT ($\rightarrow C_3H_7^+$ (90%)), accompanied by a minor ET reaction ($\rightarrow C_3H_8^+$ (10%)). The absolute efficiency of the HT reaction is found to increase significantly in passing from CH_4 (0.123) to C_2H_6 (0.327) to C_3H_8 (0.632), namely with the corresponding reaction exothermicity ($\Delta H°(CH_4) - \Delta H°(C_2H_6) = 43$ kcal mol^{-1}; $\Delta H°(C_2H_6) - \Delta H°(C_3H_8) = 20$ kcal mol^{-1}).

Unsaturated Hydrocarbons. Alkenes inefficiently incorporate an oxygen atom by reaction with HO_3^+ (H = H or D). The oxygenated product patterns depends upon the specific alkene used. Indeed, ethylene C_2H_4 ((d) in Table 2) gives rise

(61) Zappey, H. W.; Ingemann, S.; Nibbering, N. M. M. *J. Am. Soc. Mass Spectrom.* **1992**, *3*, 515.
(62) Bouma, W. J.; Nobes, R. H.; Radom, L. *Org. Mass Spectrom.* **1982**, *17*, 315.
(63) (a) Huntress, W. T., Jr.; Sen Sharma, D. K.; Jennings, K.; Bowers, M. T. *Int. J. Mass Spectrom. Ion Physics* **1977**, *24*, 25. (b) Nobes, R. H.; Radom, L. *Org. Mass Spectrom.* **1982**, *17*, 340. (c) Uggerud, E. *J. Am. Chem. Soc.* **1994**, *116*, 6873. (d) Nhuyen, M. T.; Bouchoux, G. *J. Phys. Chem.* **1996**, *100*, 2089.

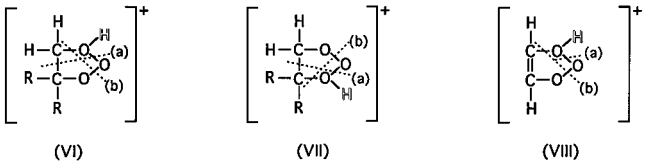

Figure 7. Proposed cyclic intermediates from the attack of HO_3^+ (H = H or D) on unsaturated substrates (ethylene (**VI** = **VII** (R = H)); allene (**VI** and **VII** (R,R = CH_2)); 1,1-difluoroethylene (**VI** and **VII** (R = F)); acetylene (**VIII**)).

to the $[H_3, C_2, O]^+$, $[H_2, H, C_2, O]^+$, $[H_4, C_2, O]^+$, $[H_3, H, C_2, O]^+$, and $[H_2, H, C, O]^+$ products, whereas allene C_3H_4 ((f) in Table 2) yields the latter two fragments. Instead, 1,1-difluoroethylene $C_2H_2F_2$ ((q) in Table 2) produces only the $[H_2, H, C, O]^+$ ion.

A unifying rationale for the above reaction patterns can be found in the tendency of HO_3^+ (H = H or D) to add to the π bond of the alkene, yielding the cyclic oxonium ions **VI** and **VII** (Figure 7), which eventually fragment after some H/H scrambling. Thus, with C_2H_4, the $[H_2, H, C, O]^+$ and $[H_4, C_2, O]^+/[H_3, H, C_2, O]^+$ products may arise from fragmentation of the intermediate **VI** = **VII** (R = H) via paths a and b, respectively. If preceded by a C-to-O(2) H transfer in **VI** = **VII**, the latter route gives rise to the $[H_3, C_2, O]^+/[H_2, H, C_2, O]^+$ pair. With allene C_3H_4, the same reaction will generate two different intermediates, i.e. **VI** (R,R = CH_2) and **VII** (R,R = CH_2). Fragmentation (a) supersedes path b in **VI** (R,R = CH_2), yielding exclusively the $[H_2, H, C, O]^+$ product. The reverse is true in **VII** (R,R = CH_2), where the only fragmentation channel is path b, preceded by a C-to-O(2) H shift. Finally, the reaction of HO_3^+ with 1,1-difluoroethylene $C_2H_2F_2$ yields predominantly the intermediate **VI** (R = F) which fragments exclusively by pathway (a) to give the $[H_2, H, C, O]^+$ ion.

A similar mechanistic model fits the oxygenated product pattern observed from the attack of HO_3^+ on acetylene C_2H_2, characterized by the predominant formation of the $[H_2, C_2, O]^+$, accompanied by minor amounts of the $[H_2, C_2, O_2]^+/[H, H, C_2, O_2]^+$ pair ((g) in Table 2). Thus, 1,2-addition of HO_3^+ to the π system of C_2H_2 leads to the formation of the cyclic oxonium ion **VIII** (Figure 7), which eventually fragments after some H/H scrambling. As for the analogous intermediates **VI** and **VII**, a favored fragmentation route is represented by pathway b, which leads to $[H_2, C_2, O]^+$. This process is accompanied by the competing fragmentation process a, which efficiently produces the $[H_2, C_2, O_2]^+/[H, H, C_2, O_2]^+$ pair.

In conclusion, the HO_3^+ ion slowly 1,2-adds to the π bond of the selected unsaturated hydrocarbons to give a cyclic intermediate which may undergo H/H scrambling before fragmentation. Both the orientation of the 1,2-addition of HO_3^+ to the π bond and the fragmentation pattern of the corresponding cyclic intermediates strongly depend on the electronic properties of the groups attached to the π system.

Carbon Monoxide. The time dependence of the ion abundances from the attack of HO_3^+ (H = H or D) on CO (3.4×10^{-8} Torr) is reported in Figure 2. The reaction pattern is characterized by the initial formation of CHO_2^+ by exothermic CO-to-O_2 ligand exchange in HO_3^+ (eq 6) ($\Delta H° = -85$ kcal mol^{-1}; $k_{obs} = 1.0 \times 10^{-10}$ cm^3 molecule^{-1} s^{-1}; eff = 0.13; $k_H/k_D = 1.0 \pm 0.2$). Step 6 is followed by a fast PT reaction between CHO_2^+ and a CO molecule to give CHO^+ ($\Delta H° = -12$ kcal mol^{-1}; $k_{obs} = 8.5 \times 10^{-10}$ cm^3 molecule^{-1} s^{-1}; eff = 1.0) (eq 7).

$$HO_3^+ + CO \rightarrow CHO_2^+ + O_2 \quad (6)$$

$$CHO_2^+ + CO \rightarrow CHO^+ + CO_2 \quad (7)$$

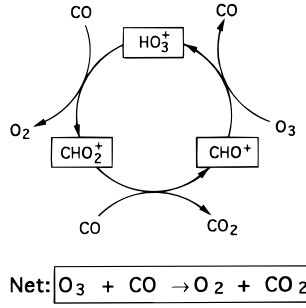

Figure 8. Gas-phase proton-catalyzed cycle of oxidation of CO to CO_2 by O_3.

Occurrence of this sequence settles the apparent discrepancy, observed in a previous study,[25] about the hardly justifiable formation of CHO^+ from attack of HO_3^+ on CO (eff = 0.18), despite PA(O_3) = 148 ± 3 kcal mol^{-1} > PA(CO) = 141.9 kcal mol^{-1}.[54,55]

Sequence 6 → 7 can be combined with the 7 ± 3 kcal mol^{-1} exothermic (and, thus, probably very fast) proton transfer from CHO^+ to O_3 to constitute the three-step acid-catalyzed cycle depicted in Figure 8.

The net result of the cycle is the oxidation of CO by O_3 to give CO_2 and O_2, regenerating the corresponding conjugated acids. The direct reaction of O_3 with CO in unobservedly slow, despite its exceedingly high exothermicity (−102 kcal mol^{-1} (if $O_2(^3\Sigma_g^-)$ is formed)).[64] Catalytic cycles in gas-phase positive ion chemistry, mostly involving transition-metal species, have recently been appearing with increasing frequency.[65] Gas-phase Fe^+-[65−67] and Mg^+-catalyzed[64] oxidations of CO to CO_2, using N_2O and O_3, respectively, as the oxygen donors, have been reported. That of Figure 8 is, to our knowledge, the first H^+-catalyzed cycle in gas-phase ion chemistry and may represent an additional source of ozone degradation in the upper atmosphere.

Reactions of $H_2{}^{16}O_3^+$ with Water ($H_2{}^{18}O$ and D_2O). Only 24% of the collisions between $[H_2{}^{16}O{\cdot}{}^{16}O_2]^+$ and $H_2{}^{18}O$ (3.8×10^{-8} Torr) are reactive (Table 5). Besides the PT ($H_3{}^{18}O^+$; 34%) and the ET ($H_2{}^{18}O^+$; 16%) products, the reaction pattern is characterized by the formation of both the $H_2{}^{16}O_2{}^{18}O^+$ (16%) and the $H_4{}^{16}O{}^{18}O^+$ ions (34%). Some indications about the most probable structure of the latter ions was obtained from their CID spectrum. The isolated $H_4{}^{16}O{}^{18}O^+$ ions lose predominantly the $H^{16}O$ fragment. This result is consistent with Gill and Radom's *ab initio* calculations at the 6-311G** level which indicate that the most stable structure of $H_4O_2^+$ is that of a tightly-bound $[H_3O{\cdot}OH]^+$ adduct.[69] The lack of an equally abundant $H^{18}O$ fragment in the $H_4{}^{16}O{}^{18}O^+$ CID spectrum speaks againts the very recent Barnett and Landman's calculations employing the BO−LSD−MD method which point to the hydrazine-like configuration $[H_2O{\cdot}OH_2]^+$ as the ground-state structure of $H_4O_2^+$.[70] In fact, the hypothetical occurrence of the symmetric $[H_2O{\cdot}OH_2]^+$ structure would allow extensive oxygen atom scrambling in $H_4{}^{16}O{}^{18}O^+$ prior to collisional fragmentation. At longer reaction times, the $[H_3{}^{18}O{\cdot}{}^{16}OH]^+$ ions further react with the bulk $H_2{}^{18}O$, yielding comparable propor-

(64) Rowe, B. R.; Fahey, D. W.; Ferguson, E. E.; Feshenfeld, F. C. *J. Chem. Phys.* **1981**, *75*, 3325.
(65) (a) Eller, K.; Schwarz, H. *Chem. Rev.* **1991**, *91*, 1121, and references therein. (b) Schroder, D.; Schwarz, H. *Angew. Chem., Int. Ed. Engl.* **1995**, *34*, 1973 and references therein.
(66) Kappes, M. M.; Staley, R. H. *J. Phys. Chem.* **1981**, *85*, 942.
(67) Kappes, M. M.; Staley, R. H. *J. Am. Chem. Soc.* **1981**, *103*, 1286.
(68) Baranov, V.; Javahery, G.; Hopkinson, A. C.; Bohme, D. K. *J. Am. Chem. Soc.* **1995**, *117*, 12801.
(69) Gill, P. M. W.; Radom, L. *J. Am. Chem. Soc.* **1988**, *110*, 4931.
(70) Barnett, R. N.; Landman, U. *J. Phys. Chem.* **1995**, *99*, 17305.

Scheme 3

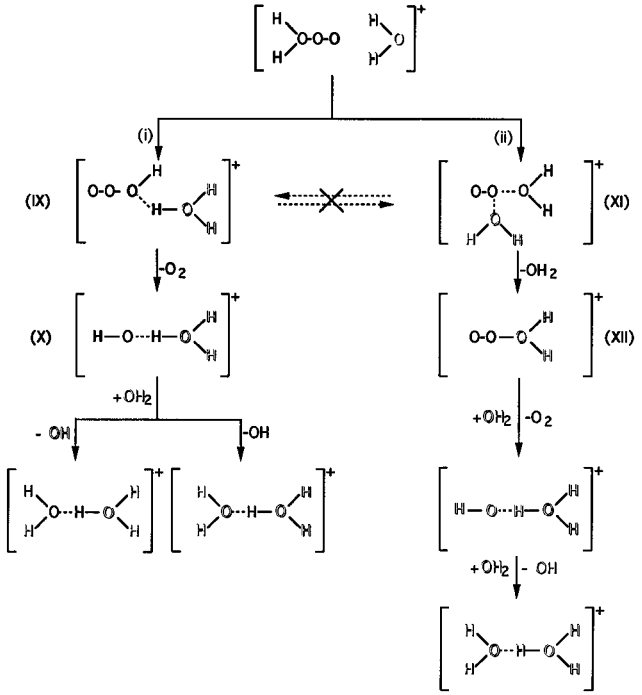

tions of the $[H_3{}^{18}O{\cdot}{}^{18}OH_2]^+$ and $[H_3{}^{18}O{\cdot}{}^{16}OH_2]^+$ products (sequence i of Scheme 3 ($H_2O = H_2{}^{18}O$)).[71] The $H_2{}^{16}O_2{}^{18}O^+$ ion **XII** (H = H; O = ^{18}O) behaves in the same way as $[H_2{}^{16}O{\cdot}{}^{16}O_2]^+$ (sequence ii of Scheme 3), in compliance with its $[H_2{}^{18}O{\cdot}{}^{16}O_2]^+$ structure. As proposed in previous related studies,[26,39−43] the relative abundances of the $[H_3{}^{18}O{\cdot}{}^{16}OH]^+$ (**X**) and the $[H_2{}^{18}O{\cdot}{}^{16}O_2]^+$ adducts (**XII**) reflect the orienting properties of $[H_2{}^{16}O{\cdot}{}^{16}O_2]^+$ ion toward the attacking $H_2{}^{18}O$ nucleophile. Thus, if hydrogen bonding between $H_2{}^{18}O$ and $[H_2{}^{16}O{\cdot}{}^{16}O_2]^+$ prevails (**IX** in Scheme 3), an exothermic ($\Delta H°$ = ca. −8 kcal mol^{-1}) PT reaction with $^{16}O_2(^3\Sigma_g^-)$ loss takes place producing $[H_3{}^{18}O{\cdot}{}^{16}OH]^+$ (**X**). If, on the contrary, the interaction occurs at the $^{16}O_2$ center of $[H_2{}^{16}O{\cdot}{}^{16}O_2]^+$ (**XI** in Scheme 3), a quasi-resonant $H_2{}^{18}O$-to-$H_2{}^{16}O$ displacement takes place yielding $[H_2{}^{18}O{\cdot}{}^{16}O_2]^+$ (**XII**). The exclusive observation of the $H_3{}^{18}O^+$ fragment from CID experiments on $[H_3{}^{18}O{\cdot}{}^{16}OH]^+$ points to the lack of any significant **IX**↔**XI** interconversion.

Attack of $[H_2O{\cdot}O_2]^+$ ions on D_2O (Scheme 3; H = D and O = ^{16}O), under exactly the same conditions, follows a reaction pattern similar to that observed in the $[H_2{}^{16}O{\cdot}{}^{16}O_2]^+/H_2{}^{18}O$ system. The overall reaction efficiency appears higher with D_2O than with $H_2{}^{18}O$ (49% vs. 24%) (Table 5). Again, the PT (41%) and the ET(22%) reactions are accompanied by formation of either $D_2O_3^+$ (7%) and $H_2D_2O_2^+$ (29%). At longer reaction times, $H_2D_2O_2^+$ further react with D_2O producing both $HD_4O_2^+$ and $H_2D_3O_2^+$ in almost equal proportions (sequence i of Scheme 3 ($H_2O = D_2{}^{16}O$)). The similar $HD_4O_2^+/H_2D_3O_2^+$ and $H_5{}^{18}O_2^+/H_5{}^{16}O{}^{18}O^+$ yield ratios measured from the reaction with H_2O of their corresponding **X** precursors (Scheme 3; $H_2O = D_2{}^{16}O$ and $H_2{}^{18}O$, respectively) suggest the lack of any appreciable hydrogen scrambling in **X** prior to its reaction with water.

(71) de Visser, S. P.; de Koning, L. J.; Nibbering, N. M. M. *J. Phys. Chem.* **1995**, *99*, 15444.

Conclusions

The thermochemistry of the HO_3^+ and $H_2O_3^+$ ions and of their neutral analogs is evaluated by measuring in a FT-ICR spectrometer the reaction efficiency of the ions toward a variety of inorganic and organic substrates with different standard ionization energy (IE) and proton affinity (PA). Analysis of the electron transfer (ET) efficiency of HO_3^+ and $H_2O_3^+$ ions allows to estimate their standard electron recombination (RE) energies as 253 ± 4 and 251 ± 3 kcal mol^{-1}, respectively. From $H°_f(HO_3^+)$ = 252 ± 3 kcal mol^{-1}, previously determined by FT-ICR bracketing techniques,[25] a value of −1 ± 5 kcal mol^{-1} is obtained for the standard heat of formation of HO_3, which is in good agreement with Schaefer and co-workers' MCHF/DZP theoretical calculations.[13] This means that, in contrast with previous theoretical indications (Table 1),[8,11,56] HO_3 is stable toward dissociation to HO($^2\Pi$) and $O_2(^3\Sigma_g^-)$ by at least 10 ± 5 kcal mol^{-1}, and therefore, its role in key ionic reactions in the upper atmosphere cannot be excluded. The measured standard RE energy of $H_2O_3^+$ ions allows us to establish a lower limit of ≥193 ± 3 kcal mol^{-1} for the standard formation enthalpy of $H_2O_3^+$. An independent estimate is based on the measure of the PA of HO_3 (167 ± 2 kcal mol^{-1}), which, coupled with the standard heat of formation of HO_3 (−1 ± 5 kcal mol^{-1}), provides a confirmatory value of 198 ± 5 kcal mol^{-1}. Collision-induced dissociation (CID) experiments on the HO_3^+ and $H_2O_3^+$ ions are consistent with the [H−O−O−O] and [H_2═O−O−O] connectivities, respectively. No evidence of a conceivable [H−O−O−O−H] connectivity was obtained for $H_2O_3^+$ ions.

The HO_3^+ ion displays a protean character by reacting with the selected substrates as Brønsted and Lewis acids, as well as an oxenium ion and an oxygen-centered free radical. Thus, HO_3^+ is able to abstract a hydride ion from most selected hydrogen donors, producing a HOOOH neutral molecule, whose formation enthalpy is estimated as ≤−26 kcal mol^{-1}. The same ion efficiently protonates substrates with PA > 150 kcal mol^{-1}, whereas it abstracts a hydrogen atom from methane and hydrazoic acid yielding the $H_2O_3^+$ product. Furthermore, HO_3^+ may add to the π-bonds of alkanes, alkenes, and acetylene, yielding a variety of oxygen-containing fragments. When all the above pathways are thermochemically precluded, as with CO, a ligand-swiching process takes place in HO_3^+ to give the CHO_2^+ ion, which may promote a three-step acid-catalyzed cycle for the O_3 oxidation of CO to CO_2 and O_2. The $H_2O_3^+$ ion, although less reactive than HO_3^+, displays a variegated chemistry as well. The most evident differences with HO_3^+ reside in the ability of $H_2O_3^+$ to protonate only substrates with PA > 165 kcal mol^{-1} and in its tendency to undergo ligand swiching by water.

Acknowledgment. This work was supported by the Ministero della Ricerca Scientifica e Tecnologica (MURST). The author expresses his gratitude to F. Cacace for his continuous support and encouragement, to F. Angelelli and A. Di Marzio for technical assistance, and to F. Grandinetti for reading the manuscript critically.

IC960549S